

Journal of Biomedical Optics

SPIEDigitalLibrary.org/jbo

Complementary fluorescence-polarization microscopy using division-of-focal-plane polarization imaging sensor

Yang Liu
Timothy York
Walter Akers
Gail Sudlow
Viktor Gruev
Samuel Achilefu

Complementary fluorescence-polarization microscopy using division-of-focal-plane polarization imaging sensor

Yang Liu,^{a,b*} Timothy York,^{c*} Walter Akers,^a Gail Sudlow,^a Viktor Gruev,^c and Samuel Achilefu^{a,b}

^aWashington University, Department of Radiology, St. Louis, Missouri 63110

^bWashington University, Department of Biomedical Engineering, St. Louis, Missouri 63110

^cWashington University, Department of Computer Science and Engineering, St. Louis, Missouri 63110

Abstract. Fluorescence microscopy offers high sensitivity for disease diagnosis. However, little structural information is revealed by this method, requiring another technique to localize the source of fluorescence. We developed a complementary fluorescence-polarization microscope. We used a division-of-focal-plane charge coupled device polarization sensor to enable real-time video rate polarization imaging without any moving parts. The polarization information provided by the microscope enabled detection of structural element and complements the fluorescence information. Application of this multimodal system for cancer imaging using a tumor selective molecular probe revealed the association of diminished structural integrity of tumor tissue with high fluorescence of the imaging agent compared to surrounding normal tissue. This study demonstrates a new paradigm to improve cancer detection and diagnosis. © 2012 Society of Photo-Optical Instrumentation Engineers (SPIE). [DOI: 10.1117/1.JBO.17.11.116001]

Keywords: fluorescence microscopy; molecular probe; near infrared; polarization microscopy; surgical margin; tumor imaging.

Paper 12499L received Aug. 6, 2012; revised manuscript received Oct. 7, 2012; accepted for publication Oct. 9, 2012; published online Nov. 1, 2012.

Pathology is the current gold standard for oncologic diagnostics. In surgical resection of tumors, the surgeon typically excises tissue close to tumor boundaries for surgical margin assessment. The specimens are subsequently analyzed offsite to ensure complete tumor removal. However, the standard staining technique used in histopathology, such as hematoxylin and eosin staining (H&E), involves lengthy procedures. Due to this time lag, surgeons occasionally complete the surgical procedure without the histopathology report, assuming that complete tumor resection was achieved. Unfortunately, some of the results can indicate positive margins, compelling the patient to undergo additional tissue resection and follow-up interventions. This poses additional pain, cost, and risk of cancer dissemination to other organs.

Fluorescence microscopy has emerged as a powerful tool for margin assessment.¹⁻⁴ The method can provide real-time assessment of samples with high detection sensitivity and specificity.^{5,6} Recent advances in fluorescence endoscopy have facilitated the real-time assessment of tissue *in vivo* as well as rapid *ex vivo* staining. Yet, the enormous advantages of fluorescence microscopy in molecular imaging and analysis are compromised by the lack of structural information. This creates practical difficulties in clinics for clinicians who rely on anatomical and structural information for disease diagnosis.

To address this challenge, we developed a complementary fluorescence-polarization microscopy system using a division-of-focal-plane polarization imaging sensor.⁷ Polarization microscopes are conventionally used to detect birefringence. In human tissues, birefringence is widely present in natural biomaterials, such as collagen fibers, and muscles. This provides the foundation

for using polarization imaging for structural assessment. Similar to whole-body multimodal imaging modalities, such as the combination of positron emission tomography (PET) with computed tomography (CT), where PET and CT provide functional and structural information, respectively, we combined fluorescence and polarization imaging techniques to provide synergistic molecular and structural information. A near infrared molecular probe, LS301, Cypate-cyclo(D-Cys-Gly-Arg-Asp-Ser-Pro-Cys)-Lys-OH, was used for tumor-selective targeted fluorescence imaging.¹

To capture the polarization information for an imaged tissue, we used a division-of-focal-plane polarimeter. These polarimeters utilize pixel-matched filters to analyze the state of polarization with high spatial and temporal resolution. In contrast, traditional polarization imaging utilizes a division-of-time approach,⁷ where samples are imaged by multiple captures through different polarization optics. The sensor used in this study⁷ is composed of a repeated filter array consisting of 0 deg, 45 deg, 90 deg, and 135 deg oriented nanowire polarization filters, which are monolithically integrated with a charge coupled device (CCD) sensor in 2-by-2 pixel blocks (Fig. 1). The filters are fabricated via a combination of interference lithography and reactive ion etching,⁸ achieving a 70 nm pitch, 140 nm height, and 140 nm period. This configuration allows for capturing the first three Stokes parameters, shown in Eq. (1), by computing directly from the measured digital values under each filtered pixel, I_x , where x represents the orientation of the pixelated linear polarization filter in degrees.

$$\begin{bmatrix} S_0 \\ S_1 \\ S_2 \end{bmatrix} = \begin{bmatrix} \frac{1}{2}(I_0 + I_{45} + I_{90} + I_{135}) \\ I_0 - I_{90} \\ I_{45} - I_{135} \end{bmatrix}. \quad (1)$$

The first Stokes parameter, S_0 , represents the total intensity and is perceived as a white light image similar to Fig. 2(a). The

*These authors contributed equally to this work.

Address all correspondence to: Samuel Achilefu, Washington University, Department of Radiology, St. Louis, Missouri 63110. Tel: 314-362-8599; Fax: 314-747-5191; E-mail: achilefu@mir.wustl.edu, Viktor Gruev, Washington University, Department of Computer Science and Engineering, St. Louis, Missouri 63110. Tel: 314-935-4465; Fax: 314-935-7302; E-mail: vgruev@wustl.edu

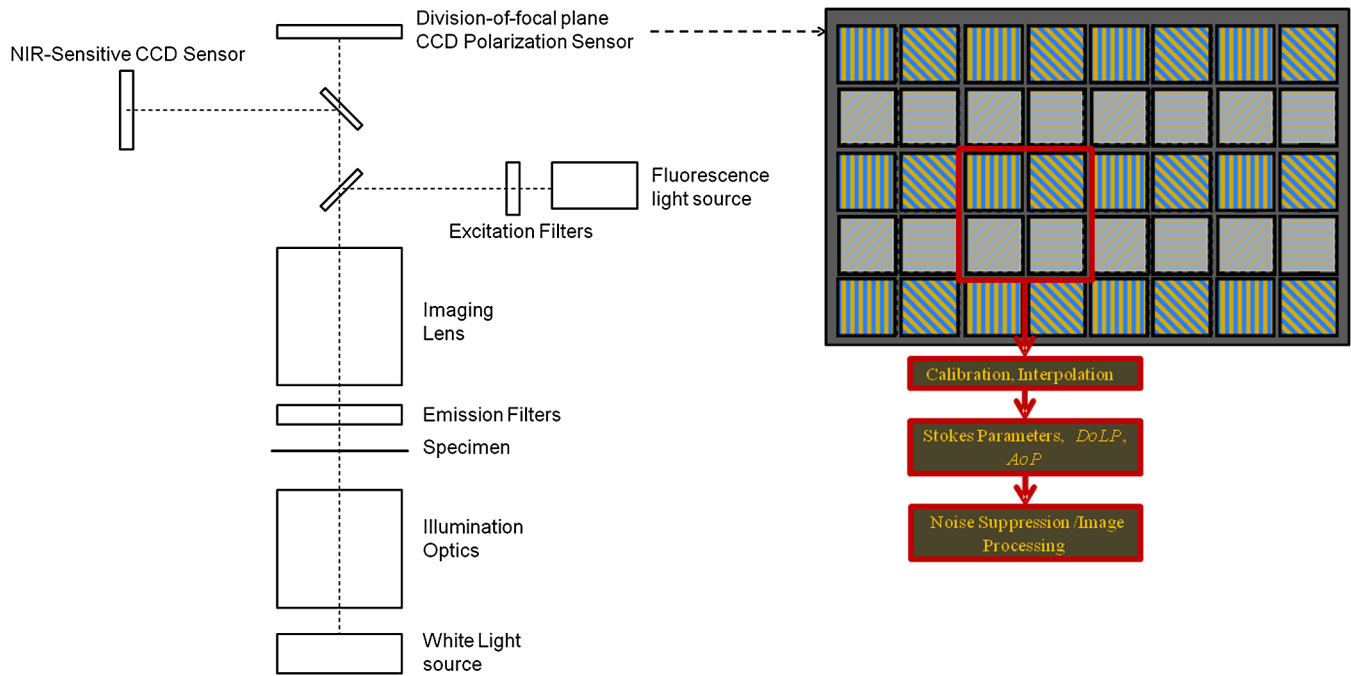


Fig. 1 Complementary fluorescence-polarization microscope with division-focal-plane polarization imaging sensor. Both real-time polarization and NIR fluorescence imaging capability are offered in this setup. The polarimeter consists of pixel matched (clockwise in red box) 0 deg, 45 deg, 90 deg, and 135 deg filters replicated across a 1 MP array. The raw frame undergoes per-pixel calibration and bicubic interpolation for each filter orientation, followed by the polarization processing and postfiltering.

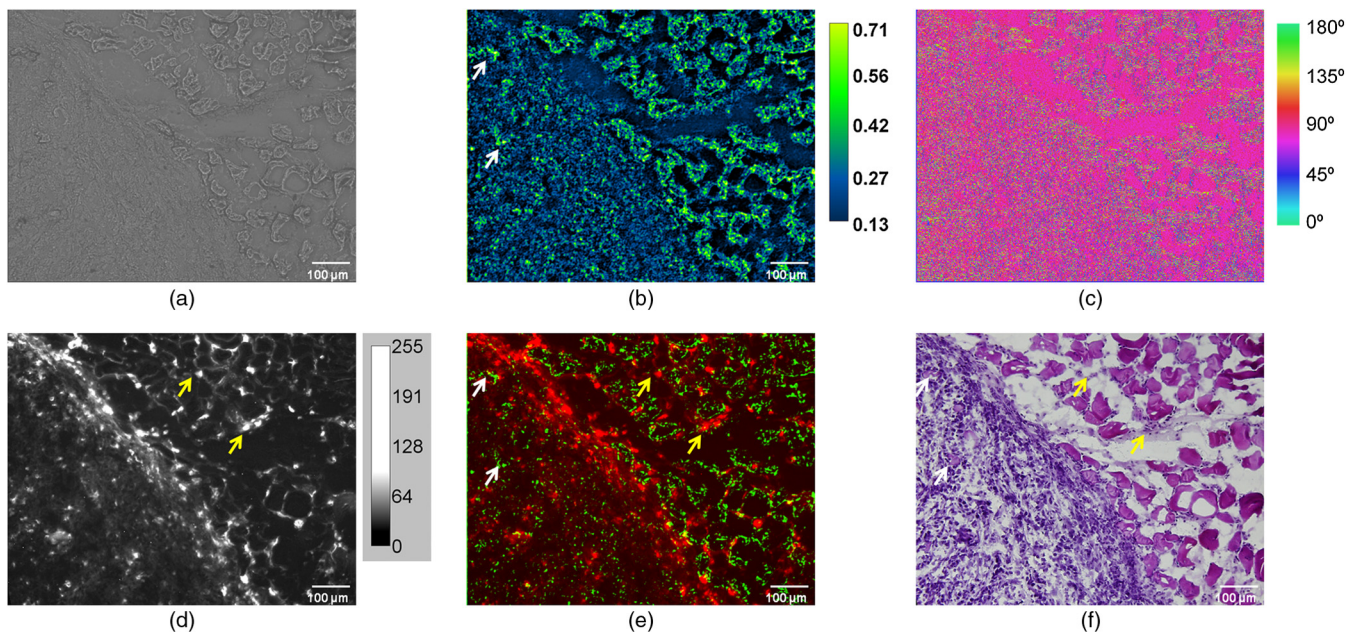


Fig. 2 Complementary microscopy for surgical margin assessment. (a) White light, (b) degree of linear polarization, (c) angle of polarization, (d) NIR fluorescence, (e) composite image of DoLP and fluorescence, and (f) H&E stained color images. The DoLP image differentiated normal tissues from tumor tissues, as evidenced by the higher DoLP signal (>0.5) in normal tissues compared to lower signal (<0.25) in tumor tissue. The fluorescence image outlines tumor tissues. White arrows indicate remnant normal tissues within tumors; yellow arrows indicate tumor tissues invading into normal tissues.

second Stokes parameter, S_1 , shows how much light is polarized in the horizontal/vertical direction, and the third Stokes parameter, S_2 , describes how much light is polarized in the ± 45 -deg direction. To compensate for nonuniformity in the filters across the imaging array, a gain and offset per pixel are used to calibrate the image⁹ before computation of the three Stokes parameters. The first three Stokes parameters allow estimation of the state of linear polarization of the region of interest. Primarily,

this is expressed in the degree of linear polarization (DoLP), a measure of how linearly polarized the viewed sample is, and the angle of polarization (AoP), which describes the primary orientation of the light. They are computed in Eqs. (2) and (3):

$$\text{DoLP} = \frac{\sqrt{S_1^2 + S_2^2}}{S_0}, \quad (2)$$

$$\text{AoP} = \frac{1}{2} \tan^{-1} \left(\frac{S_2}{S_1} \right). \quad (3)$$

The sensor is a megapixel array, which operates at 40 frames per second and has extinction ratios of ~ 60 , with a dynamic range of 65 dB and maximum signal-to-noise ratio of 45 dB. Detailed sensor specifications can be found elsewhere.¹⁰ To the best of our knowledge, this is the first time that such a sensor has been applied to biomedical applications.

The multimodal optical design is illustrated in Fig. 1. Both fluorescence imaging and polarization imaging are enabled for real-time microscopy. The optical setup is developed from the Olympus BX51. In the current setup, a near infrared (NIR)-sensitive CCD sensor (Olympus DP71) is used for fluorescence imaging, which delivers optimal performance at 830 nm channel. The white light image, degree of polarization, angle of polarization images are displayed in the graphical user interface in real time.

In this study, we used the new method to assess the tumor margins of mice mammary carcinoma (4T1). This invasive tumor serves as a good model for the current study because of its ability to infiltrate surrounding normal tissue, which simulates clinical conditions. The complementary microscope provides fast and convenient pathological assessment of tissues (Fig. 2). The DoLP image readily identified the inhomogeneous distribution of polarization information at the tumor boundaries. The normal tissues (muscles) showed a higher degree-of-linear-polarization than the tumors, allowing structural differentiation between the two tissue types [Fig. 2(b) and 2(e)]. In addition, the DoLP image also resolved the normal remnant structure elements within the tumors [Fig. 2(b) and 2(e)]. Based on the DoLP image, a first-pass screening of tissues could be accomplished. With molecular probe LS301, the status of tumor boundaries

were assessed [Fig. 2(d) and 2(e)]. The fluorescent contrast outlined tumor tissues, including those that invaded into the surrounding tissues. However, the lack of structural contrast in the fluorescence image confounded analysis of the tumor distribution relative to normal tissue. With a combination of both the fluorescence and polarization contrasts [Fig. 2(e)], the tumor density in the region of interest was readily visualized. Compared to the gold standard H&E staining, which provides absorption-based contrast [Fig. 2(f)], the multimodal microscopy provides [Fig. 2(e)] contrast based on functional and structural characteristics, which represent discernible complementary imaging contrast for tumor detection and localization.

Beyond simple tumor detection, the new method can also be applied to assess the severity of cancer invasion. This is illustrated in Fig. 3, where tumor, muscle, and connective tissues were all present (Fig. 3). At the borders of three different tissue types, tumors were accurately highlighted by the fluorescence contrast. In contrast, normal muscles and connective tissues exhibited higher DoLP, but negligible fluorescence signal, than tumors. Based on the complementary microscopy, regions 1, 2, 3, and 4 have cancer invasion in descending order (Fig. 3). The complementary contrast mechanisms provided by the new system amplified the differences between tumors and surrounding tissues, facilitating medical diagnosis. Interestingly, visualization of the cancer invasion using the standard H&E images provided only moderate contrast. Guided by the fluorescence-polarization images, a close examination of the H&E image agrees well with the multimodal imaging data.

In the current setup, two sensors are used for optimal performance in the NIR spectral window. The current polarization imaging sensor has an NIR-cut filter that hinders it from offering desirable performance at NIR range. In a future study, we will fabricate an NIR-optimized polarization sensor to enable

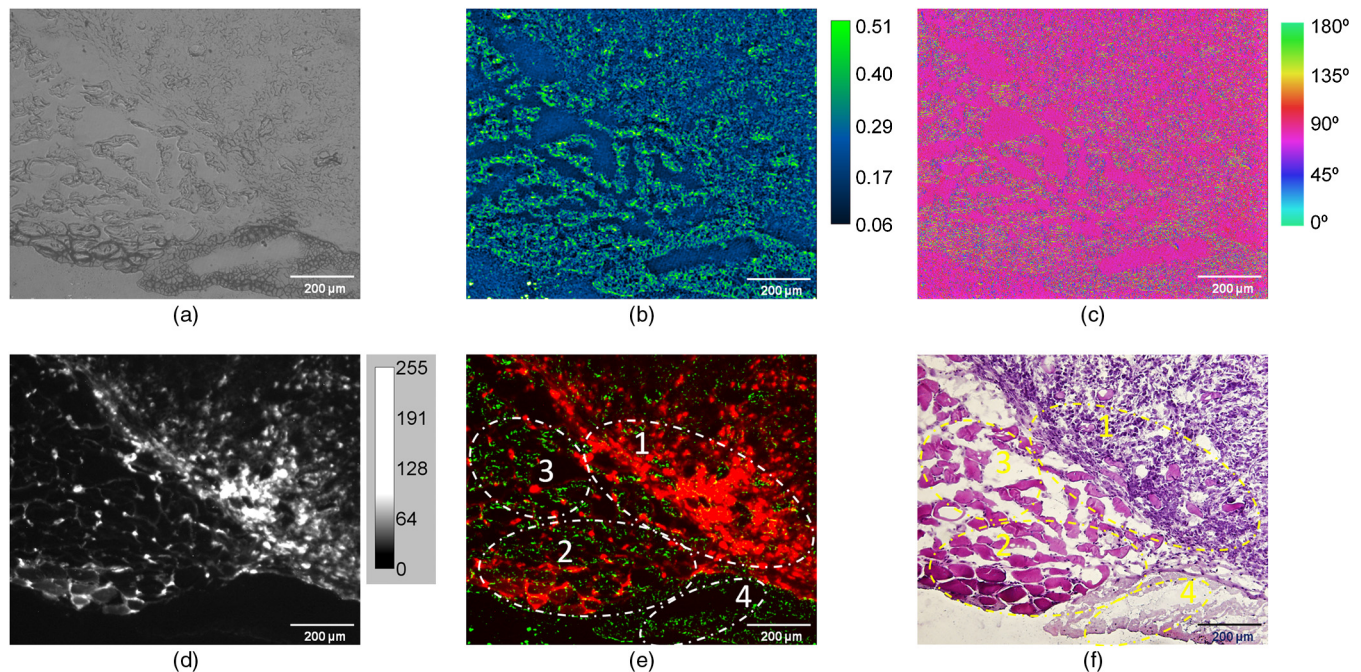


Fig. 3 Severity of cancer invasion assessed by complementary multimodal microscopy. (a) White light, (b) degree of linear polarization, (c) angle of polarization, (d) NIR fluorescence, (e) composite image of DoLP and fluorescence, and (f) H&E stained color images. Circles with dash lines outline several areas with different severity of cancer invasions. In (e), regions with a higher degree of cancer invasion exhibited higher fluorescence signal and lower DoLP signal than normal tissue, and vice versa (Region 1 > Region 2 > Region 3 > Region 4). In (f), cancer invasion is evidenced by high cellular density, pleomorphism and epithelial inclusion. Image (e) correlates well with (f).

multimodal imaging with a single sensor and allow bona fide image co-registration. For the division-of-focal-plane technique, presence of interpolation artifacts remains a challenge that needs remedies. Based on our previous analysis, we concluded that bicubic spline interpolation can achieve the best performance.¹¹ In the current study, the removal of interpolation artifacts is further enhanced by spatial filtering, which is enabled by fast Fourier transform (FFT). A Gaussian band-pass filter was employed, removing ultra-high frequency components, which primarily arise from interpolation artifacts.

In this study, we have demonstrated the initial concept of fluorescence-polarization microscopy for surgical margin assessments. In future studies, the fluorescence and polarization signals could be calibrated to generate standard chart for quantitative measurement of cancer invasion, facilitating cancer staging. Similarly, many other pathological examinations can be explored with this new technique. Compared to other emerging histological techniques, such as confocal microscopy, two-photon fluorescent microscopy and single harmonic generation, the method reported herein allows for wide-field real-time imaging within a large field of view, which is the key for rapid histopathological assessment of tissue samples. Although the current setup is designed and tested in *ex vivo* settings, a similar concept can be extended to intravital and dissection microscopy. Although we used the tumor-targeted NIR molecular probe, LS301, for the fluorescent contrast, other cancer-targeting imaging agents may be also used in future studies. For example, molecular probes with diverse targeting mechanisms and spectra characteristics may be used to augment the utility of fluorescence microscopy in the clinical settings. The real-time feature of polarization contrast provides cross-validation and structural reference for fluorescence contrast.

In this study, the polarization contrast is primarily based on the DoLP because the AoP did not reveal seemingly useful diagnostic information. A comprehensive study is needed to evaluate the utility of AoP in tissue analysis. Successful interpretation of AoP may provide additional beneficial information for complementary microscopy. Here, the image co-registration of fluorescent and polarization contrast was performed offline using the ImageJ software. We expect to rectify this limitation in future studies by processing the data online.

In conclusion, we have developed a complementary fluorescence-polarization microscope using a division-of-focal-plane polarization imaging sensor, for the first time. The new method

enabled real-time wide-field multimodal microscopy without any moving parts. It facilitated surgical margin assessment in the mouse mammary carcinoma. Cancer invasion was visualized and evaluated. This new method may be applied to other medical applications. Intravital microscopes and microendoscopes based on this technique may be developed in the future, extending its utility to diverse *in vivo* applications.

Acknowledgments

This study was supported in part by grants from the National Institutes of Health (NIBIB R01 EB008111 and NCI R01 CA171651; SA), as well as the Air Force Office of Scientific Research (FA9550-10-1-0121 and FA9550-12-1-0321; VG). We thank Mrs. Kexian Liang for preparing LS301.

References

1. Y. Liu et al., "Hands-free, wireless goggles for near-infrared fluorescence and real-time image-guided surgery," *Surgery* **149**(5), 689–698 (2011).
2. S. Keereweer et al., "Image-guided surgery in head and neck cancer: current practice and future directions of optical imaging," *Head Neck* **34**(1), 120–126 (2012).
3. G. Themelis et al., "Enhancing surgical vision by using real-time imaging of alphavbeta3-integrin targeted near-infrared fluorescent agent," *Ann. Surg. Oncol.* **18**(12), 3506–3513 (2011).
4. J. R. van der Vorst et al., "Near-infrared fluorescence imaging of liver metastases in rats using indocyanine green," *J. Surg. Res.* **174**(2), 266–271 (2012).
5. S. Achilefu, "Lighting up tumors with receptor-specific optical molecular probes," *Technol. Cancer Res. Treat.* **3**(4), 393–409 (2004).
6. Y. Urano et al., "Rapid cancer detection by topically spraying a gamma-glutamyltranspeptidase-activated fluorescent probe," *Sci. Transl. Med.* **3**(110), 110–119 (2011).
7. V. Gruev, R. Perkins, and T. York, "CCD polarization imaging sensor with aluminum nanowire optical filters," *Opt. Express* **18**(18), 19087–19094 (2010).
8. V. Gruev, "Fabrication of a dual-layer aluminum nanowires polarization filter array," *Opt. Express* **19**(24), 24361–24369 (2011).
9. T. York and V. Gruev, "Calibration method for division of focal plane polarimeters in the optical and near-infrared regime," *Proc. SPIE* **8012**, 80120H (2011).
10. T. York and V. Gruev, "Characterization of a visible spectrum division-of-focal-plane polarimeter," *Appl. Opt.* **51**(22), 5392–5400 (2012).
11. S. Gao and V. Gruev, "Bilinear and bicubic interpolation methods for division of focal plane polarimeters," *Opt. Express* **19**(27), 26161–26173 (2011).